The Impact of Weightbearing CT on Understanding Midfoot Charcot Deformities

Abstract

Introduction: Charcot neuroarthropathy (CN) is a severe condition often associated with diabetic neuropathy, leading to significant foot deformities. This study aims to compare the accuracy of traditional radiographs and weightbearing computed tomography (WBCT) in evaluating foot alignment in midfoot Charcot deformities.

Methods: This retrospective study included 19 adult diabetic patients (23 feet) with midfoot Charcot deformities who underwent WBCT at the Duke Orthopedic Department. Demographic data, clinical history, and radiographic evaluations were collected. Key radiographic parameters were compared between radiographs and WBCT. Advanced WBCT-specific measurements, such as Foot and Ankle Offset (FAO), Forefoot Arch Angle, Sinus Tarsi Impingement, Subfibular Impingement, and Medial Facet Subluxation, were analyzed.

Results: The mean age of patients was 64 years, with a mean BMI of 35.1 kg/m². Distribution of Charcot deformities showed Type I (Lisfranc pattern) as the most common (43.48%). Comparison of angles revealed that the lateral column height was significantly lower in WBCT (mean 12.26 mm) compared to radiographs (mean 19.12 mm) ($p = 0.000$). Subfibular impingement was the only parameter significantly correlated with the Lew Schon classification ($p = 0.007$), with more proximal deformities showing lower impingement values.

Conclusion: The significant finding of lower lateral column height in WBCT suggests a higher risk of ulceration in more lateral collapsed cases, indicating the need for earlier intervention. The correlation between subfibular impingement and Lew Schon classification emphasizes WBCT's potential in aiding precise surgical planning and improving patient outcomes. WBCT provides valuable insights into the structural changes in midfoot Charcot deformities.

Keywords: Charcot neuroarthropathy, Weightbearing computed tomography (WBCT), Midfoot deformities, Subfibular impingement

Introduction

Charcot neuroarthropathy (CN) is a chronic disease that results in the loss of bone architecture in the foot due to bone fragmentation[1–3]. This condition occurs because of neuropathy, which involves damage to the peripheral nerves, leading to a loss of sensation and proprioception. It is hypothesized that neurovascular alterations and microtrauma play significant roles in its pathogenesis [3,4]. Consequently, progressive foot destabilization occurs, exacerbated by repeated pressure on the feet during walking. Without appropriate intervention, it can result in severe deformities and functional disability.

A prevalence ranging from 0.1% and 0.9% has been reported [5,6]. Diabetic Neuropathy (DN) serves as a common etiology of Charcot neuroarthropathy, emerging as a late complication of diabetes. DN affects between 0.15% and 2.5% of individuals with diabetics, particularly those who with disease duration exceeding 10 years, regardless of whether it is Type 1or Type 2 [3]. However, CN has been associated with many conditions including syphilis, congenital neuropathy, Guillain-Barré syndrome, chronic alcoholism, leprosy, syringomyelia, toxic exposure, poliomyelitis, spinal cord injury, multiple sclerosis, and renal transplantation surgery [2].

The midfoot is the most affected region of the foot, ranging from 60-90% of the cases in the literature, corresponding to the Brodsky type 1 and 2 classification of Charcot foot disease [7–10]. Lew Schon proposed a classification system, categorizing midfoot Charcot into four distinct types based on the affected area: Type I, the Lisfranc pattern; Type II, the naviculocuneiform/ metatarsocuboid pattern; Type III, the perinavicular pattern; and Type IV, the transverse tarsal pattern[11,12].

Evaluating radiographs of these deformities is critical to determine the correct treatment. Patients with significant midfoot deformities often exhibit pronounced abduction of the forefoot and a foot shape resembling a rocker bottom, which increases the risk of ulceration at the bottom of the collapsed arch [13]. Additionally, the impact of these deformities on the alignment and stability of the hindfoot remains unclear. Therefore, thorough radiographic assessment is essential for accurate diagnosis and treatment planning, ensuring that appropriate interventions are implemented to address both the midfoot

deformities and any potential consequences on hindfoot alignment and stability[10,11].

The weightbearing computed tomography (WBCT) is a valuable diagnostic tool that enables us to evaluate the foot in a standing position [14–16]. This allows for a comprehensive assessment of the Charcot collapsed foot, revealing the relationship between the bones of the midfoot and hindfoot, as well as the contact between bone prominences and the floor [17,18]. By providing detailed three-dimensional imaging, assists surgeons in developing tailored treatment strategies to address the specific needs of each patient.

The objectives of this study are to compare the accuracy of radiographic parameters for foot alignment between traditional radiographs and weightbearing computed tomography (WBCT). Additionally, the study aims to evaluate the behavior of hindfoot joints in patients with midfoot collapsed Charcot, with the goal of understanding the role of WBCT in the evaluation of these patients.

Methods

This study was a retrospective study conducted at DUKE Orthopedic Department, a tertiary care center specializing in foot and ankle disorders. The study was conducted from February to May of 2024.

We included adult diabetic patients (≥18 years) diagnosed with midfoot Charcot deformities who presented to our clinic previously of the study period and underwent to undergo weightbearing CT (WBCT) to evaluate their midfoot deformities. A total of 19 patients (23 feet) met the inclusion criteria and were included in the study.

At baseline, we collected from medical records the demographic data (age, sex, bone mass index), clinical history (side of deformity, history of ulcer, and presence of diabetic retinopathy – DR, peripheral vascular disease – PVD, and chronic kidney disease - CKD) and use of insulin.

All participants underwent standard radiographic evaluation and WBCT of the affected foot. Bilateral standing WBCT scans were conducted at the DUKE Orthopedic Department using a cone-beam WBCT scanner (PedCAT©, Curvebeam©, Hatfield, Pennsylvania, USA). The raw 3D WBCT data was reconstructed into sagittal, coronal, and axial images using specific software (CubeView©, Curve-Beam©, Hatfield, Pennsylvania, USA). Semi-automated 3D measurements were performed using Disior Bonelogic© Ortho Foot and Ankle Software (version 2.1.4; Helsinki, Finland).

Radiographic measures were taken to compare to WBCT images[11,19]. These measures included: (1) Talar-first metatarsal angle on lateral view, (2) Medial column height, (3) Lateral column height, (4) Calcaneal-fifth metatarsal angle on lateral view, (5) Talar-first metatarsal angle on anteroposterior (AP) view and (6) Talonavicular coverage angle on AP view.

The primary outcome was the severity of midfoot Charcot deformities, classified according to Schon's classification[12] (Figures 1-4). Secondary outcomes included foot and ankle alignment measures derived from WBCT, such as the hindfoot alignment angle, midfoot height, and forefoot arch angle. Adhering to previously published protocols and original descriptions [20–22], a total of 12 variables were measured at the WBCT images: (1) Talar-first metatarsal angle on lateral view, (2) Medial column height, (3) Lateral column height, (4) Calcaneal-fifth metatarsal angle on lateral view, (5) Talar-first metatarsal angle on anteroposterior (AP) view, (6) Talonavicular coverage angle on AP view, (7) Foot and Ankle offset, (8) Forefoot arch angle, (9) Sinus tarsi impingement, (10) Subfibular impingement, (11) Medial facet subluxation, and (12) percentage of medial facet uncoverage.

We used descriptive statistics to summarize baseline characteristics of the cohort. Continuous variables were expressed as means and standard deviations, and categorical variables as frequencies and percentages. Comparisons between groups were made using t-tests for continuous variables and chi-square tests for categorical variables. Additionally, analysis of variance (ANOVA) was performed to assess differences in continuous variables across different locations of Charcot deformities.

Results

Nineteen adult diabetic patients (≥18 years) diagnosed with midfoot Charcot deformities were included in the study, totaling 23 feet that met the inclusion criteria. The mean age of the patients was 64 years (standard deviation (SD): 10.1), and the mean body mass index (BMI) was 35.1 kg/m² (SD: 6.6). Among the participants, nine were male (47.4%) and ten were female (52.6%).

The distribution of Charcot deformities according to the Lew Schon classification among the 23 affected feet was as follows: Type I (Lisfranc pattern) was the most common, observed in 10 feet (43.48%). Type II (naviculocuneiform/metatarsocuboid pattern) was present in 3 feet (13.04%),

Type III (perinavicular pattern) in 7 feet (30.43%), and Type IV (transverse tarsal pattern) in 3 feet (13.04%).

The ANOVA results indicated that there was no statistically significant difference in BMI and age among the different locations of Charcot deformities ($p = 0.869$ and $p = 0.646$, respectively).

Chi-square tests were conducted to evaluate the association between categorical variables (sex, insulin use, history of ulcer, chronic kidney disease, diabetic retinopathy, and peripheral vascular disease) and the location of Charcot deformities and the analysis showed no significant association for any of the variables (Table 1).

The results comparing angles measured on radiographs and WBCT images are summarized in Table 2. The medial column height, calcaneal-fifth metatarsal angle, talar-first metatarsal angle in the AP and lateral view, and talonavicular coverage angle showed no statistically significant differences between radiographs and WBCT, indicating that these angles are comparable across imaging modalities. However, the lateral column height differed significantly between radiographs and WBCT, with radiographs showing a mean of 19.12 (SD = 5.82) and WBCT showing a mean of 12.26 (SD = 3.65) ($p = 0.000$).

Advanced measurements were conducted using WBCT including Foot and Ankle Offset (FAO), Forefoot Arch Angle, Sinus Tarsi Impingement, and the Percentage of Medial Facet Uncoverage, which did not show significant differences across different locations of midfoot Charcot deformities. However, subfibular impingement demonstrated a statistically significant difference according to the Lew Schon classification ($p = 0.007$) (Table 3).

To evaluate the relationship between Lew Schon's classifications and subfibular impingement, an ANOVA test was performed, which revealed a negative coefficient (-0.8394). This finding suggests that a more proximal focus of the deformity is associated with an average decrease of 0.9 mm in subfibular impingement measurement ($p = 0.029$).

Discussion

Our research results indicate that the alignment angles of the foot, as measured radiographically, can be similarly assessed using WBCT images, with comparable results. The exception was the lateral column height, which showed

lower values in the WBCT images. Furthermore, when evaluating the specific measures obtained from WBCT, we found that only subfibular impingement was statistically related to the Lew Schon classification, suggesting that the more proximal the deformity, the lower the value of the subfibular impingement.

The anatomic classification introduced by Brodsky' divided the deformities into four types and the Type 1 is a midfoot deformity, known to be the most common, affecting about 70% of all cases [23]. The location of the deformity in our sample is quite different from the initial description by Lew Schon [12] . According to the radiographic mapping, most of our patients had the Type I pattern, at the Lisfranc joint, rather than the naviculocuneiform/metatarsocuboid pattern described in Schon's paper.

The reliability of the angle measurements in the radiographs and WBCT was similar, as expected, since the measurement technique was well described by Gould [19] and Schon [12]. However, we found that the lateral column height was significantly lower in the WBCT than in the radiographs. This could be a valuable measure in the WBCT, as we all know that the risk of ulceration is higher in those with the most lateral collapsed cases [12]. Consequently, those patients may be considered eligible for earlier intervention to avoid poorer prognosis.

The use of WBCT in the context of foot and ankle disorders has provided new perspectives for understanding these diseases and deformities [15]. New parameters were developed that can only be measured on WBCT images, such as Foot and Ankle Offset [24], Forefoot arch angle [25], Sinus tarsi impingement [26], Subfibular impingement [26], and Medial facet subluxation [27]. However, the only measure that shown a correlation with the Lew Schon Classification in this study was the Subfibular impingement. This finding suggests that more proximal deformities have the fibula closer to the calcaneus. Since it is often challenging to distinguish the structures of the midfoot after Charcot destruction, this bone impingement may indicate higher talonavicular abduction angles [26], and this information can assist surgeons in better planning the surgical intervention.

This study has several strengths, notably being the first known study to use WBCT for advanced measurements of foot alignment in patients with midfoot Charcot deformities. The detailed analysis of specific variables, such as subfibular impingement and the more accurate lateral column height, adds significant value to the understanding of these deformities. However, the study has some limitations, including a relatively small sample size, which may affect

the generalizability of the results. Additionally, the retrospective nature of the study may introduce potential selection biases. Future studies should focus on larger sample sizes to confirm these findings and on prospective designs to evaluate the progression of midfoot Charcot deformities using WBCT.

In conclusion, our study highlights significant findings from using WBCT in evaluating midfoot Charcot deformities. The lateral column height was significantly lower in WBCT images compared to radiographs, and subfibular impingement was the only parameter significantly correlated with the Lew Schon classification, with more proximal deformities showing lower subfibular impingement values. These insights demonstrate WBCT's potential to reveal critical structural changes in midfoot Charcot deformities, aiding in precise surgical planning and improved patient outcomes.

References

[1] Safavi PS, Jupiter D, Panchbhavi V. A Systematic Review of Current Surgical Interventions for Charcot Neuroarthropathy of the Midfoot. The Journal of Foot and Ankle Surgery : Official Publication of the American College of Foot and Ankle Surgeons 2017. https://doi.org/10.1053/j.jfas.2017.06.011.

[2] Madan SS, Pai DR. Charcot Neuroarthropathy. Orthop Surg 2013;5:86–93. https://doi.org/10.1111/os.12032.

[3] Trieb K. The Charcot foot: pathophysiology, diagnosis and classification. Bone Jt J 2016;98-B:1155–9. https://doi.org/10.1302/0301-620x.98b9.37038.

[4] Jeffcoate WJ. Charcot foot syndrome. Diabetic Medicine : A Journal of the British Diabetic Association 2015;32:760–70. https://doi.org/10.1111/dme.12754.

[5] McInnes AD. Diabetic foot disease in the United Kingdom: about time to put feet first. J Foot Ankle Res 2012;5:26. https://doi.org/10.1186/1757-1146-5-26.

[6] Kaynak G, Birsel O, Güven MF, Öğüt T. An overview of the Charcot foot pathophysiology. Diabet Foot Ankle 2013;4:21117. https://doi.org/10.3402/dfa.v4i0.21117.

[7] Ferreira RC, Gonçalez DH, Filho JMF, Costa MT, Santin RAL. MIDFOOT CHARCOT ARTHROPATHY IN DIABETIC PATIENTS: COMPLICATION OF AN EPIDEMIC DISEASE. Rev Bras Ortop (Engl Ed) 2012;47:616–25. https://doi.org/10.1016/s2255-4971(15)30013-6.

[8] Sella EJ, Barrette C. Staging of charcot neuroarthropathy along the medial column of the foot in the diabetic patient. J Foot Ankle Surg 1999;38:34–40. https://doi.org/10.1016/s1067-2516(99)80086-6.

[9] BRODSKY JW, ROUSE AM. Exostectomy for Symptomatic Bony Prominences in Diabetic Charcot Feet. Clin Orthop Relat Res 1993;296:21–6. https://doi.org/10.1097/00003086-199311000-00005.

[10] El-Mowafi H, Elghazy MA, Kandil YR, Ali S, El-Hawary A, Abulsaad MS. Charcot Arthropathy of Foot and Ankle: Radiographic and Clinical Patterns with Related Outcomes. Int Orthop 2021;45:2201–8. https://doi.org/10.1007/s00264-021-05082-6.

[11] Schon LC, Easley ME, Cohen I, Lam PW-C, Badekas A, Anderson CD. The Acquired Midtarsus Deformity Classification System—Interobserver Reliability and Intraobserver Reproducibility. Foot Ankle Int 2002;23:30–6. https://doi.org/10.1177/107110070202300106.

[12] Schon LC, Weinfeld SB, Horton GA, Resch S. Radiographic and Clinical Classification of Acquired Midtarsus Deformities. Foot Ankle Int 1998;19:394–404. https://doi.org/10.1177/107110079801900610.

[13] Pinzur MS, Schiff AP. Deformity and Clinical Outcomes Following Operative Correction of Charcot Foot: A New Classification With Implications for

Treatment. Foot & Ankle International 2017;5:107110071774237. https://doi.org/10.1177/1071100717742371.

[14] Pavani C, Belvedere C, Ortolani M, Girolami M, Durante S, Berti L, et al. 3D measurement techniques for the hindfoot alignment angle from weight-bearing CT in a clinical population. Sci Rep 2022;12:16900. https://doi.org/10.1038/s41598-022-21440-9.

[15] Barg A, Bailey T, Richter M, Netto C, Lintz F, Burssens A, et al. Weightbearing Computed Tomography of the Foot and Ankle: Emerging Technology Topical Review. Foot & Ankle International 2017:107110071774033. https://doi.org/10.1177/1071100717740330.

[16] Rojas EO, Mansur NS, Dibbern KN, Auch EC, Schmidt E, Vivtcharenko V, et al. Weightbearing Computed Tomography for Assessment of Foot and Ankle Deformities: The Iowa Experience. Foot Ankle Orthop 2022;7:2473011421S00419. https://doi.org/10.1177/2473011421s00419.

[17] Ranjit S, Sangoi D, Cullen N, Patel S, Welck M, Malhotra K. Assessing the coronal plane deformity in Charcot Marie Tooth Cavovarus feet using automated 3D measurements. Foot Ankle Surg 2023;29:511–7. https://doi.org/10.1016/j.fas.2023.02.013.

[18] Belvedere C, Giacomozzi C, Carrara C, Lullini G, Caravaggi P, Berti L, et al. Correlations between weight-bearing 3D bone architecture and dynamic plantar pressure measurements in the diabetic foot. J Foot Ankle Res 2020;13:64. https://doi.org/10.1186/s13047-020-00431-x.

[19] Gould N. Graphing the Adult Foot and Ankle. Foot Ankle Int 1982;2:213–9. https://doi.org/10.1177/107110078200200407.

[20] Cody EA, Williamson ER, Burket JC, Deland JT, Ellis SJ. Correlation of Talar Anatomy and Subtalar Joint Alignment on Weightbearing Computed Tomography With Radiographic Flatfoot Parameters. Foot Ankle Int 2016;37:874–81. https://doi.org/10.1177/1071100716646629.

[21] Kunas GC, Probasco W, Haleem AM, Burket JC, Williamson ERC, Ellis SJ. Evaluation of peritalar subluxation in adult acquired flatfoot deformity using computed tomography and weightbearing multiplanar imaging. Foot Ankle Surg 2018;24:495–500. https://doi.org/10.1016/j.fas.2017.05.010.

[22] Netto C de C, Shakoor D, Dein EJ, Zhang H, Thawait GK, Richter M, et al. Influence of investigator experience on reliability of adult acquired flatfoot deformity measurements using weightbearing computed tomography. Foot Ankle Surg 2019;25:495–502. https://doi.org/10.1016/j.fas.2018.03.001.

[23] Brodsky J. The Diabetic Foot. In: Haskell A, Coughlin MJ, editors. Coughlin and Mann's Surgery of the Foot and Ankle. 10th ed., Philadelphia, PA: Elsevier; 2023.

[24] Lintz F, Ricard C, Mehdi N, Laborde J, Bernasconi A, Richardi G, et al. Hindfoot alignment assessment by the foot–ankle offset: a diagnostic study. Arch Orthop Trauma Surg 2023;143:2373–82. https://doi.org/10.1007/s00402-022-04440-2.

[25] Ferri M, Scharfenberger AV, Goplen G, Daniels TR, Pearce D. Weightbearing CT Scan of Severe Flexible Pes Planus Deformities. Foot Ankle Int 2008;29:199–204. https://doi.org/10.3113/fai.2008.0199.

[26] Jeng CL, Rutherford T, Hull MG, Cerrato RA, Campbell JT. Assessment of Bony Subfibular Impingement in Flatfoot Patients Using Weight-Bearing CT Scans. Foot Ankle Int 2019;40:152–8. https://doi.org/10.1177/1071100718804510.

[27] Netto C de C, Godoy-Santos AL, Saito GH, Lintz F, Siegler S, O'Malley MJ, et al. Subluxation of the Middle Facet of the Subtalar Joint as a Marker of Peritalar Subluxation in Adult Acquired Flatfoot Deformity: A Case-Control Study. J Bone Jt Surg 2019;101:1838–44. https://doi.org/10.2106/jbjs.19.00073.

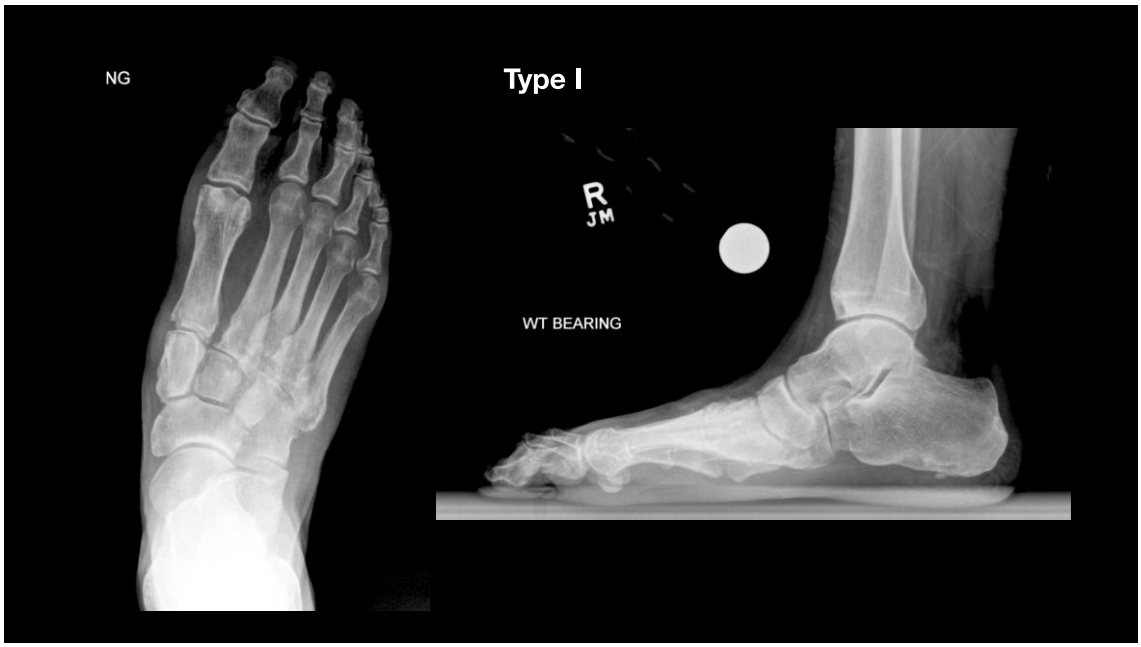

Figure 1 – Midfoot Charcot Lew Schon Type I

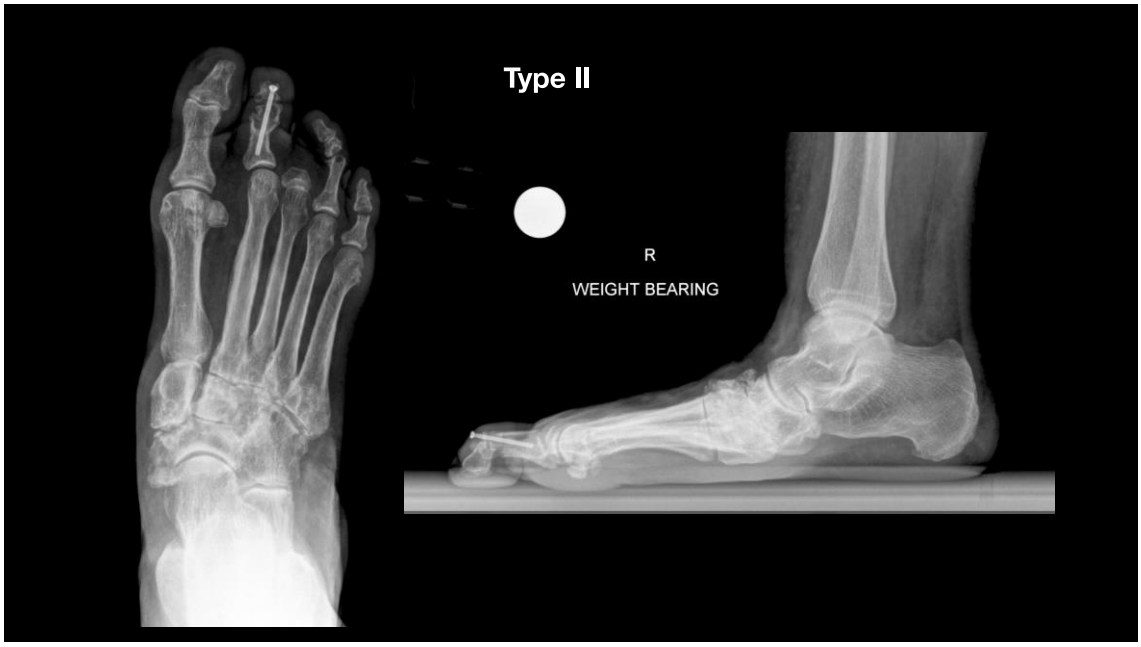

Figure 2 – Midfoot Charcot Lew Schon Type II

Figure 3 – Midfoot Charcot Lew Schon Type III

Figure 4 – Midfoot Charcot Lew Schon Type IV

Table 1 - Distribution of Categorical Variables by Lew Schon Classification

	Lew Schon Classification				p-value
	I	II	III	IV	
Sex					
Male	2	1	4	3	
Female	8	2	3	0	0.079
Insulin use					
Yes	2	0	3	1	
No	8	3	4	2	0.502
History of ulcer					
Yes	2	1	2	2	
No	8	2	5	1	0.494
CKD					
Yes	1	1	2	0	
No	9	2	5	3	0.542
DR					
Yes	2	1	1	0	
No	8	2	6	3	0.739
PVD					
Yes	2	2	3	2	
No	8	1	4	1	0.322

CKD: Chronic Kidney Disease; **DR**: Diabetic Retinopathy; **PVD**: Peripheral Vascular Disease

Table 2 - Comparison of Angles Measured on Radiographs and WBCT

	Radiographs		WBCT			
Measurement	Mean	SD	Mean	SD	Mean difference	p-value
Medial Column Height	17.41	8.46	16.97	7.31	0.44	0.665
Calcaneal-Fifth Metatarsal Angle	9.04	11.06	9.57	10.39	-0.52	0.645
Lateral Column Height	19.12	12.26	12.26	3.65	6.86	0.000
Talar-First Metatarsal Angle (AP)	30.52	10.03	30.04	8.24	0.48	0.758
Talar-First Metatarsal Angle (lateral)	20.09	11.68	16.50	13.70	3.59	0.132
Talonavicular Coverage Angle	16.46	17.71	14.27	13.07	2.20	0.363

WBCT, weightbearing computed tomography; **SD**, standard deviation; **AP**, anteroposterior.

Table 3 - Results of WBCT measures by Lew Schon Classification

Lew Schon Classification	FAO	Forefoot Arch Angle	Sinus Tarsi Impingement	Subfibular Impingement (mm)	Medial Facet Uncoverage (%)
I - Lisfranc pattern	2.91	0.31	1.27	4.94	27.05
II - naviculocuneiform/ metatarsocuboid pattern	1.20	1.40	1.09	2.12	33.27
III - perinavicular pattern	3.38	9.03	0.30	4.41	37.23
IV - transverse tarsal	8.20	3.90	0.00	1.23	47.90
Mean	5.00	3.33	0.81	3.91	33.52
p-value	0.410	0.321	0.114	0.007	0.816

FAO: Foot and Ankle Offset.